Measurement of the second virial coefficient for the interaction of dilute colloidal particles in a mixed solvent

M. L. Kurnaz and J. V. Maher
Department of Physics and Astronomy, University of Pittsburgh, Pittsburgh, Pennsylvania 15260
(Received 7 June 1996; revised manuscript received 15 August 1996)

Colloidal suspensions of charge-stabilized polystyrene latex spheres in near-critical mixtures of 2,6-lutidine and water aggregate reversibly on the side of the coexistence curve rich in the nonpreferred liquid. We have used static light scattering and a Zimm analysis to determine the second virial coefficient B_2 for this system. Measurements were made as a function of temperature for different solvent compositions. On the aggregation side of the coexistence curve, as the temperature is brought near but not into the aggregation zone, the virial coefficient plunges through zero to large, negative values. On the nonaggregating side of the coexistence curve, the virial coefficient drops to a small negative value very close to coexistence. On the critical trajectory we have observed similar behavior of the virial coefficient to that seen on the aggregating side even though aggregation does not occur on this thermodynamic trajectory. We have also used lower surface charge density particles where the aggregation occurs on the opposite side of the coexistence curve. The results are similar to those just described for the high surface charge density particles. The combined evidence points to a gradual and continuous change in solvent fluctuation-colloidal particle interaction near the solvent coexistence curve, as solvent composition is varied through the critical composition. [S1063-651X(96)02212-X]

PACS number(s): 68.45.Gd, 64.70.Ja, 78.35.+c, 82.70.Dd

I. INTRODUCTION

Colloidal particles in mixed solvents can show reversible aggregation in the one-phase regime of the mixture near the mixture's phase separation temperature [1–5]. This aggregation condition has been shown to be related to the affinity of the colloidal surfaces for one of the solvent components [4,5]. In particular, for a 2,6-lutidine plus water (LW) mixture with colloidally dispersed polystyrene latex spheres (PLS) in a temperature range near the critical temperature T_c in the mixture's two-phase region, the particles will partition into one of the solvent phases, with the meniscus between the liquid phases clear to the eye and showing no sign of population by colloidal particles. Which phase of the solvent attracts the particles depends on the surface charge density of the particles, with high surface charge density particles preferring the water-rich phase and low charge density particles preferring the lutidine rich phase. As temperature is advanced deeper into the two-phase region (all effects discussed here are equilibrium effects), there is a temperature T_W at which particles appear on the meniscus (most particles remain in the preferred phase, whose population depletion is too small to measure). T_W changes with the surface charge density of the particles [4], but not with radius or with number density of the particles in the sample. The aggregation observed in the one-phase region [5] is then restricted to the side of the solvent's coexistence curve poor in the component which is rich in the partitioning-favored phase.

In a recent paper [6], we have reported a measurement of the second virial coefficient B_2 for colloidal particle interactions in the nonaggregating, one-phase temperature regime as the aggregation temperature of one of our samples was approached. For our very dilute colloids whose departures from ideal gas behavior are small, this virial coefficient carries the information on the sign and importance of any weak interparticle interactions. While there were some puzzling features involving the magnitude of the virial coefficient, Ref. [6] showed a dramatic change in the interparticle interactions, from strongly repulsive at temperatures far from the aggregation point T_a to strongly attractive at the temperatures nearest to T_a (obviously once the aggregation temperature is reached no equilibrium measurement of the interparticle interaction is possible). On the thermodynamic trajectory reported in Ref. [6], the change of sign of B_2 from repulsive to attractive interactions occurred at a temperature 1 K away from T_a.

In this paper we report the measurement of B_2 as a function of temperature on a variety of thermodynamic trajectories, two of which never touch the aggregation zone (one of these on the critical composition of the mixed solvent) and one of which approaches the aggregation zone which has been shifted to the opposite side (from Ref. [6]) of the solvent coexistence curve by changes in the surface processing of the colloidal particles. The interest in observing these additional thermodynamic trajectories is both to compare relative magnitudes of attraction strength and to gain insight into whether the apparently abrupt transition from aggregating to nonaggregating behavior as solvent composition is varied results from an abrupt or continuous variation of the net attractive interaction.

II. EXPERIMENTAL DESIGN AND DATA ANALYSIS

As in our earlier work [4–7], dilute suspensions of well-characterized, monodisperse PLS (Interfacial Dynamics, Portland, OR) in near-critical mixtures of 2,6-lutidine (Aldrich Chemical, Milwaukee, WI) and water (LW) were studied. PLS was prepared using a surfactant-free emulsion-polymerization technique, where stabilization against aggregation is provided by a net surface charge density of several $\mu C/cm^2$ sulfonated end groups preferentially located

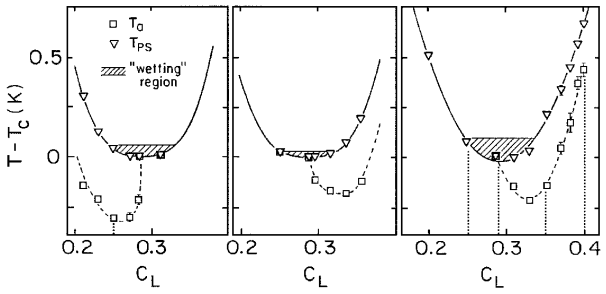

FIG. 1. Measured difference of phase separation temperature (▽) T_{ps}, and aggregation temperature (□) T_a, from the critical temperature T_c, vs solvent composition c_L. Also shown are the coexistence curve (solid line), the aggregation curve, (dashed line, drawn to guide the eye), and expected complete wetting region (hashed region, from Ref. [9]). Particle types are left, $d=0.371\pm0.02$ μm, $\sigma=0.38$ μC/cm^2; middle, $d=0.378\pm0.06$ μm, $\sigma=3.85$ μC/cm^2; right, $d=0.555\pm0.03$ μm, $\sigma=5.70$ μC/cm^2. The vertical dotted lines on the figure show the trajectories reported on in this work.

on the surface of the sphere.(We use surface charge density as measured by titration as a measure of sulfonic groups available on the surface for solvation. The actual surface charge density should depend on the local solvent composition near the particle surface and has not been measured in this experiment.)

In our earlier work [4,5] we measured the onset of the aggregation zone T_a. Figure 1 shows the results of those measurements for PLS particles of several surface charge densities, as well as the measured phase separation temperature T_{ps} at each of the solvent compositions used (at each point in Fig. 1 when the T_a and T_{ps} symbols overlap, no aggregation was observed). It is worth mentioning that the LW system has a lower consolute point.

In the present study, samples were made with a wide variety of colloidal volume fraction, two different kinds of PLS and at various different solvent compositions. Table I lists all the samples reported in this paper. Static light scattering was measured as a function of wave number and number density of colloidal particles at each of a variety of temperatures for each of the samples. In our earlier work [4,5] we have observed aggregation over a much wider range of colloidal volume fractions, but the most reliable light scattering results were obtained for colloid particle volume fractions reported herein for each sample. Below these concentrations the colloidal-particle light scattering signal becomes too weak for accurate separation from the solvent-fluctuation signal, and far above this concentration multiple scattering poses a problem. Accordingly the quantitative results presented below were all obtained in the range favorable to light scattering. In addition, measurements were made at one temperature for a series of samples of varying colloidal particle density in pure water for purposes of calibration.

TABLE I. The samples used for the second virial coefficient measurements.

Type	$d(\mu\text{m})$	$\sigma(\mu\text{C/cm}^2)$	C_L	ϕ
A	0.555 ± 0.03	5.70	0.224	$3\times10^{-7}-3\times10^{-6}$
A	0.555 ± 0.03	5.70	0.287	$1\times10^{-6}-8\times10^{-6}$
A	0.555 ± 0.03	5.70	0.350	$3\times10^{-7}-3\times10^{-6}$
A	0.555 ± 0.03	5.70	0.400	$3\times10^{-7}-3\times10^{-6}$
B	0.345 ± 0.02	0.33	0.250	$1\times10^{-6}-8\times10^{-6}$

The colloidal particle radius was chosen large enough that it was much larger than the correlation length for solvent fluctuations throughout the range of our measurements. It was then possible to subtract the essentially flat Lorentzian background scattering from solvent fluctuations and treat the remaining scattering $I_{ex}(\theta)$ as pure colloidal-particle scattering. This colloidal scattering $I_{ex}(\theta)$ could then be written as

$$I_{ex}(\theta)=NS(\theta)P(\theta), \tag{1}$$

where $P(\theta)$ is the form factor for the scattering of a beam of intensity I_0 from an isolated colloidal particle, $S(\theta)$ is the structure factor which carries all the information about correlations among colloidal particles, and N is the number density of colloidal particles.

The scattered light intensity at $\theta=0°$ is only a function of the number density of the particles and the structure factor $S(0)$, i.e.,

$$I_{ex}(0)=NS(0)K, \tag{2}$$

where [8]

$$K=P(0)=\frac{32\pi^4R^6|m^2-1|^2}{9\lambda^4r^2}I_0. \tag{3}$$

We can also rewrite this equation in a more useful form as

$$\frac{1}{S(0)}=\frac{K}{I_{ex}(0)}N. \tag{4}$$

In the dilute colloid limit where the colloidal particles might be expected to approach ideal gas behavior, the density expansion of the zero-wave-number limit of the structure factor can meaningfully be truncated to retain only the first term correcting the ideal gas approximation, the term containing B_2, the second virial coefficient

$$\frac{1}{S(0)}=1+\frac{2NB_2}{N_A}, \tag{5}$$

where N_A is Avogadro's number, and

$$B_2(T)=2\pi N_A\int_0^\infty[1-e^{-U(r)/kT}]r^2dr, \tag{6}$$

where r is the distance between the particles, and $U(r)$ is the interaction potential.

Having established the relation between the static light scattering and the second virial coefficient we turn our attention to the extrapolation of $S(q)$ to determine $S(0)$, where we made use of a Zimm analysis. This analysis allows us to extract the structure factor $S(q)$ from the measured intensities $I(\theta)$ where $q=(4\pi n/\lambda)\sin(\theta/2)$ is the wave vector of the scattering. In this experiment we have the advantage that we are performing our measurements at extraordinarily small

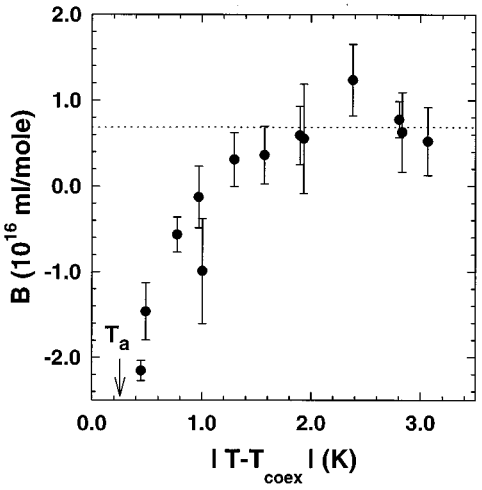

FIG. 2. Temperature dependence of the measured second virial coefficient for $\sigma = 5.70\ \mu\text{C/cm}^2$ at $c_L = 0.35$. The horizontal dotted line shows the value of the measured virial coefficient for the pure-water calibration samples. The arrow indicates the temperature T_a at which aggregation sets in.

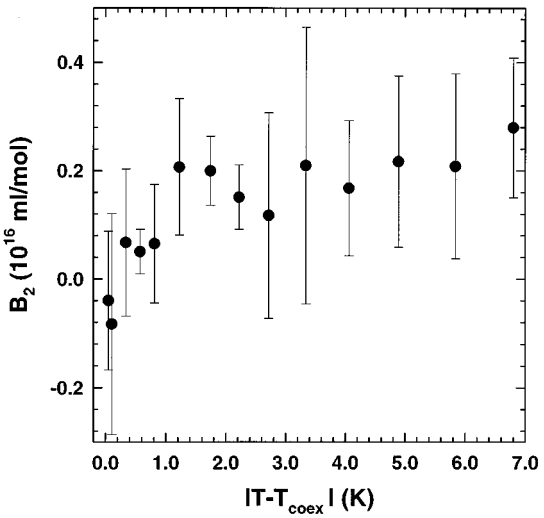

FIG. 3. Temperature dependence of the measured second virial coefficient for $\sigma = 5.70\ \mu\text{C/cm}^2$ at $c_L = 0.224$.

values of the colloidal-particle number density; such small values that reasonable estimates of the q and N dependence of the structure factor in the region of the first form factor maximum should have their first q-dependent terms of order 10^{-5}, if we assume a hard-core potential for the PLS in water and expand $S(q)$ in terms of q. As was discussed in Ref. [6], we do not understand the origin of the simultaneous appearance of the very small q dependence exhibited by the data and the very large N dependence presented below. The effect is, however, very reproducible.

Figure 2 shows the previously reported [6,7] virial coefficients for the high surface charge density PLS ($\sigma = 5.70\ \mu\text{C/cm}^2$) on the aggregating side of the aggregation curve ($c_L = 0.350$) as a function of the absolute temperature difference from the coexistence temperature for that solvent composition. In addition, a horizontal line shows the value of the measured virial coefficient for the pure-water sample.

As was noted above, the present experiment supplements the data of Fig. 2 by extending the measurements to other thermodynamic trajectories and to particles with opposite solvent affinities. The behavior of the virial coefficient on the nonaggregating side of the coexistence curve ($c_L = 0.224$) can be seen in Fig. 3. The virial coefficient shows no decrease as the temperature approaches the coexistence curve until the temperature is brought within 1 K of T_C, and even near T_C the observed negative values of the virial coefficient are compatible with zero (no interaction) or a slightly attractive interaction, but in any case are much smaller in magnitude than in the preceding (aggregating) case.

The measured virial coefficients for the same PLS on the critical trajectory ($c_L = 0.287$) are shown on Fig. 4. We have never observed aggregation on the critical trajectory in any of our earlier measurements. However, the virial coefficients show somewhat similar behavior to that seen for the aggregating sample in Fig. 2, with smaller magnitudes in the apparently attractive region (and somewhat larger uncertainties near T_C, as critical opalescence forces a larger subtraction for solvent composition fluctuations in the data analysis).

As was noted above, in our earlier measurements [4,5] we observed that the low surface charge density PLS ($\sigma = 0.33\ \mu\text{C/cm}^2$) aggregate on the water-rich side of the coexistence curve. Figure 5 shows the result of virial coefficient measurements on the aggregating side ($c_L = 0.250$) for these low surface charge density spheres. The behavior is quite similar to the high surface charge density spheres on their aggregating side of the coexistence curve, with the attractive region confined to a narrower temperature zone but with a large magnitude virial coefficient in this zone.

As discussed in our earlier work [6,7], the magnitude of the virial coefficient deep in the repulsive regime is very large. If one naively modeled the particles as hard spheres, this magnitude would correspond to a hard sphere radius of $R = 4.2\ \mu\text{m}$, roughly ten times the radius of the particles and

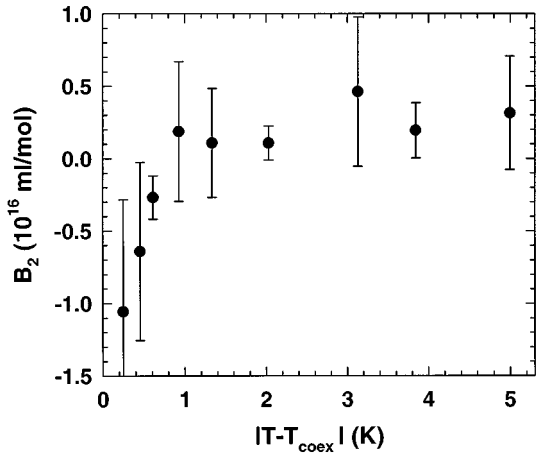

FIG. 4. Temperature dependence of the measured second virial coefficient for $\sigma = 5.70\ \mu\text{C/cm}^2$ at $c_L = 0.287$ (critical).

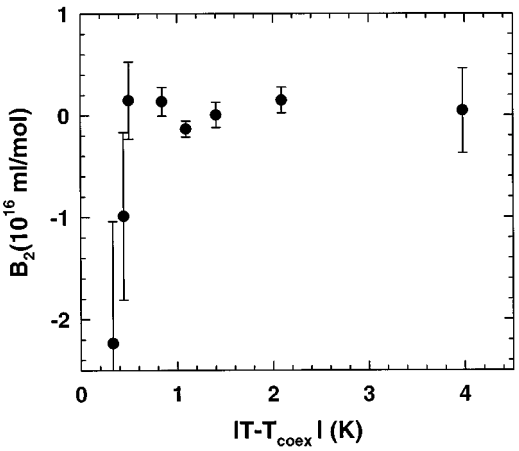

FIG. 5. Temperature dependence of the measured second virial coefficient for $\sigma = 0.33\ \mu C/cm^2$ at $c_L = 0.250$.

comparable to the average interparticle spacing. A hard sphere model with a repulsive-core radius of two particle radii (0.6 μm) should be plausible in this case, since no reasonable estimate of the Debye screening length allows that length to be comparable to the colloidal particle size. Using the published electrolytic dissociation constant for 2,6-lutidine [9], in our earlier paper we estimated the Debye screening length to be 7–10 nm [5]. This large-apparent-radius effect has been measured by Philipse and Vrij in a different system and treated with a speculation that the spheres interact significantly over distances of several radii [10]. Similarly, Thirumalai [11] found a need to set the effective hard sphere radius of colloidal particles to the mean interparticle distance in his calculations in order to explain colloidal crystallization at observed volume fractions.

If we restrict our discussion to ignore the long-range repulsion and look for inconsistency with the assumption that the temperature-dependent reduction of the virial coefficient results from solvent-composition fluctuations, it seems reasonable to crudely model the attraction as arising when the surfaces of two particles are separated by only a few solvent correlation lengths ξ. Figure 6 shows the correlation lengths measured for the trajectories mentioned above. Using these correlation lengths at each $|T-T_{coex}|$ and choosing 10 correlation lengths arbitrarily as the maximum range of a plausible overlap of adsorption layers, it is instructive to define a potential

$$U(r) = \begin{cases} \infty & r < 2R \\ -U_0 & 2R < r < 2R + 10\xi \\ 0 & r > 2R + 10\xi . \end{cases} \tag{7}$$

The value of U_0 needed to reproduce the virial coefficient nearest the point of aggregation for each of the three trajectories on which aggregation occurs is approximately 12 kT. On the critical trajectory and the other nonaggregating trajectory, the value of U_0 at the point closest to the solvent's coexistence curve is approximately 9 kT. These interaction energies are fairly insensitive to the arbitrary choice of the range of the potential, namely, doubling or decreasing this range by half changes the energies mentioned above by less than 10%. Also if we use this simple model potential for higher $|T-T_{coex}|$ we observe that the required well depth to obtain the measured virial coefficient gets smaller as we move away from the aggregation region. Given the simplicity of this model and the wide variation (3 − 30 nm) of the correlation lengths at the end points of the measured trajectories, the consistency of the well depths is striking. The small but consistent difference of model well depths on different trajectories suggests that the energetics underlying the reversible aggregation involve continuous changes of free energy across the entire range of temperature and solvent composition and no abrupt change at the point of aggregation.

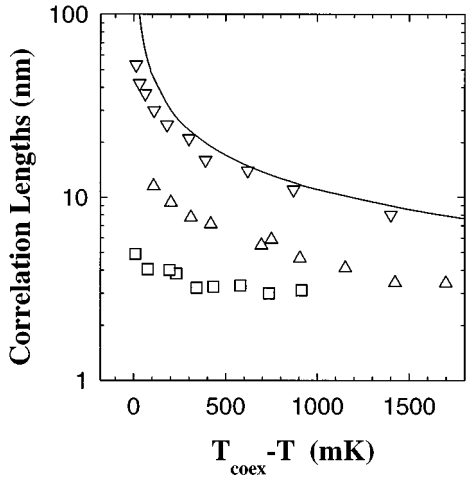

FIG. 6. Variation of the measured correlation length for solvent-composition fluctuation ξ with temperature $|T-T_{coex}|$, for $c_L = 0.25$ (△), $c_L = 0.35$ (▽), and $c_L = 0.40$ (□). Also shown is the correlation length for the critical composition (solid line, from Ref. [4]).

III. SUMMARY AND CONCLUSIONS

We have measured second virial coefficients for very dilute colloidal dispersions of charge-stabilized polystyrene latex spheres in the one-phase region of the mixed solvent 2,6-lutidine plus water on thermodynamic trajectories known to vary the appearance of aggregation and the importance of critical effects. These measurements were made as a function of temperature for PLS of two different surface charge densities and various solvent compositions. The temperature ranges started deep in the one-phase region and approached the coexistence curve. Far from the coexistence curve, all of the systems showed similar behavior, with virial coefficients large and positive, indicating significant repulsion at a much longer range than would be expected from the known particle diameter and any reasonable estimate of the Debye screening length. As the temperature is brought nearer, but definitely not into, the aggregation zone, on the aggregating side of the coexistence curve and on the critical trajectory, the virial coefficient plunges through zero to large negative (attractive interaction) values, whereas on the nonaggregating side the virial coefficient remains positive until the coexistence curve is nearly reached. These results suggest that a

mere change from repulsion to attraction is not enough for aggregation, and aggregation sets in at much larger, negative values of the second virial coefficient, hence, a much stronger attraction between the particles. While no aggregation has been observed on the critical trajectory, a simple calculation shows that the strength of attractive interaction is only slightly reduced in comparison with the aggregating case. Further, on the noncritical, nonaggregating trajectory a significant reduction of repulsion was observed, even though attractive effects never became sufficiently strong to produce aggregation. The evidence thus points to a gradual and continuous change in solvent-fluctuation–colloidal-particle interaction near the coexistence curve as solvent composition is varied through the critical composition.

This work was supported by the U.S. Department of Energy through Grant No. DE-FG02-84ER45131.

[1] D. Beysens and D. Estève, Phys. Rev. Lett. **54**, 2123 (1985).
[2] V. Gurfein, F. Perrot, and D. Beysens, Phys. Rev. A **40**, 2543 (1989).
[3] J. S. van Duijneveldt and D. Beysens, J. Chem. Phys. **94**, 5222 (1991).
[4] P. D. Gallagher, Ph.D. thesis, University of Pittsburgh, 1991; P. D. Gallagher and J. V. Maher, Phys. Rev. A **46**, 2012 (1992).
[5] P. D. Gallagher, M. L. Kurnaz, and J. V. Maher, Phys. Rev. A **46**, 7750 (1992).
[6] M. L. Kurnaz and J. V. Maher, Phys. Rev. E **51**, 5916 (1995).
[7] M. L. Kurnaz, Ph.D. thesis, University of Pittsburgh, 1994.
[8] H. C. van de Hulst, *Light Scattering by Small Particles* (Dover, New York, 1981).
[9] K. H. Hellwege, A. M. Hellwege, K. Schäfer, and E. Lax, *Eigenschaften der Materie in ihren Aggregatzuständen* (Springer-Verlag, Berlin, 1960).
[10] A. P. Philipse and A. Vrij, J. Chem. Phys. **88**, 6459 (1988).
[11] D. Thirumalai, J. Phys. Chem. **93**, 5637 (1989).